ACS Sustainable Chemistry & Engineering

Research Article

pubs.acs.org/journal/ascecg

Production of DMC from CO_2 via Indirect Route: Technical–Economical–Environmental Assessment and Analysis

Lorena F. S. Souza,[†] Priscila R. R. Ferreira,[†] José Luiz de Medeiros,*[,†] Rita M. B. Alves,[‡] and Ofélia Q. F. Araújo[†]

[†]Escola de Química, Federal University of Rio de Janeiro, Av. Pedro Calmon, 550, Cidade Universitária, Rio de Janeiro 21941-901, Brazil

[‡]Braskem S.A., Pinheiros, 05425-070 São Paulo, Brazil

Supporting Information

ABSTRACT: Interest in dimethyl carbonate (DMC), a saleable chemical destination of CO_2, has grown significantly. DMC is an oxygenated octane-booster and a safer and nontoxic substitute of well-established methylating-carbonylating hazardous chemicals like dimethyl sulfate and phosgene. Considering the CO_2 routes to DMC, the one commercially promising converts CO_2 with ethylene oxide (EO) to ethylene carbonate (EC), which then reacts with excess methanol (MeOH) to DMC and ethylene glycol (EG). This indirect route (IR) apparently exhibits green chemistry attributes. It converts greenhouse gases (GHG) to valuables, such as EG, EC, and DMC. Apparently, it is not energy intensive; it has 100% atom economy without wastes. However, there is a massive energetic obstacle occluded in the separation of the azeotropic pair DMC–MeOH yet to be considered. This work assesses the technical, economical, and environmental IR flowsheet for CO_2 conversion to DMC. Assessment of entrainers for extractive distillation of DMC–MeOH was accomplished for EG versus methyl–isobutyl–ketone. Process design, energy consumption, and GHG emissions were assessed and showed that both alternatives are profitable but gave negative chemical sequestration indexes. Their GHG emissions through energy consumption and purges overcome the chemical conversion of CO_2 to DMC. The process alternative using EG as the entrainer exhibits higher profitability and better sustainability indexes.

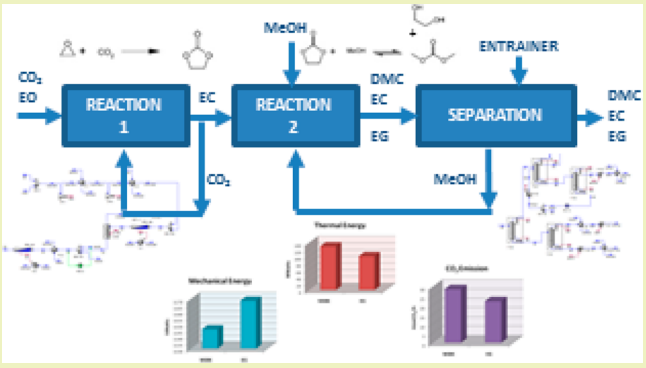

KEYWORDS: *CO_2 reutilization, CO_2 to DMC, DMC, Extractive distillation, MIBK, Ethylene glycol, GHG chemical sequestration*

INTRODUCTION

Dimethyl carbonate (DMC) is a biodegradable and nontoxic chemical that is feasible as a environmentally acceptable chemical destination of greenhouse gas (GHG) CO_2.[1] DMC is a chemical exempt from VOC classification (in the United States) that can be used as raw material for producing valuable chemicals including aromatic polycarbonate and has also qualified as an octane booster.[2,3] The spectrum of potential applications of DMC showed substantial enlargement in recent years, particularly in connection with its use as a green substitute for well-established methylation and carbonylation of extremely hazardous agents like phosgene and dimethyl sulfate.[4]

In recent decades, much has been discussed about ways to counterbalance the negative effects of GHG atmospheric accumulation. A considered alternative involves the establishment of a new category of sustainable chemical routes with one or more of the following attributes: no production of deleterious wastes, no GHG emissions, utilization of renewable raw materials, optimum use of energy and resources, and potential to convert problematic wastes of other industries to harmless useful commodities. In this category, one may include processes that convert GHG CO_2 to tradable goods.[5] Figure 1a presents some examples of chemicals that can be produced from CO_2. Another sustainable solution for minimizing GHG emissions and stabilization of atmospheric CO_2 is its destination to geological formations that can hold massive inventories of CO_2. The CO_2 tripod, capture– transport–geological storage, is based on the principle of "return the carbon back into the ground".[6] However, suchan alternative does not add value to CO_2, aggregating only capital and operating expenditures without revenues. Therefore, alternatives that add value to CO_2—displacing it from the category of waste to the status of raw material—should be explored. This is the case of production of DMC from CO_2.

Special Issue: Sustainable Chemical Product and Process Engineering

Received: August 5, 2013
Revised: October 6, 2013
Published: October 27, 2013

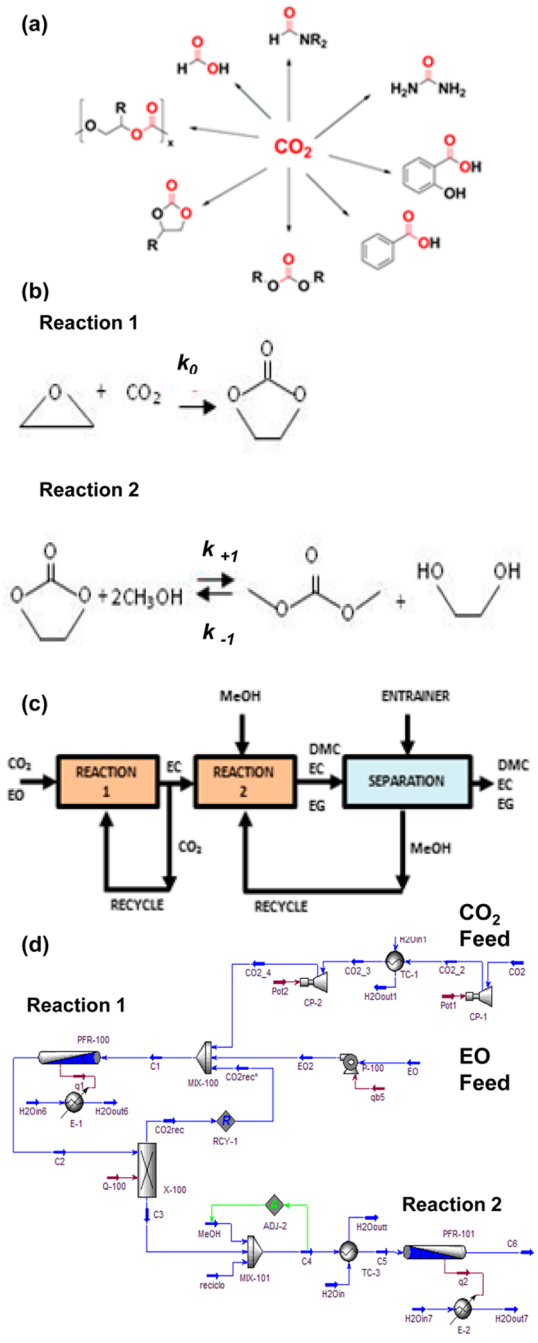

Figure 1. (a) Chemicals potentially produced from CO_2. (b) Two-step indirect route (IR) to DMC. (c) Process for DMC production via IR. (d) Reaction section of IR to DMC.

For large-scale production of DMC from CO_2, one route seems to be promising: the indirect route (IR) for two-step conversion of CO_2 with ethylene oxide (EO) to ethylene carbonate (EC), which then reacts with excess methanol (MeOH) giving DMC and ethylene glycol (EG) as shown in Figure 1b. Figure 1c depicts a block diagram of IR, while Figure 1d shows the simulation flowsheet for the reaction section of IR. IR exhibits several green chemistry attributes. IR converts a major GHG to valuable EG, EC, and DMC. Apparently, IR is not energy intensive; IR has 100% atom economy and does not generate wastes.[1] Furthermore, IR aims at replacing the traditional DMC production route with phosgene, a hazardous chemical in terms of health, safety, and environment (HSE). However, IR has to face an energetic obstacle occluded in the separation of the azeotropic pair DMC−MeOH. This energetic penalty should be carefully considered and circumvented, if possible, in order to make IR workable. This work conducts a technical−economical−environmental assessment of the IR processes for CO_2 conversion to DMC. Assessment of entrainers for energy and HSE effective extractive distillation of DMC−MeOH was accomplished for EG versus methyl−isobutyl−ketone (MIBK) alternatives. Process flowsheets were simulated with ASPEN−HYSYS to assess design, energy consumption, and GHG emissions.

METHODOLOGY

Process Diagram for Indirect Route (IR). The DMC production by IR is well discussed in the literature.[1,4,5,7] For the purpose of quantitative assessment of IR, reaction kinetic formulas are needed in order to predict the impact of operating conditions on reaction yield, separation costs, and economic response. As shown in Figure 1c and d, IR is designed with two serial reactor systems followed by a separation section. The reaction section must be examined and integrated to the separation section, seeking a design structure that attains a compromise between their often conflicting requirements and targets. The basis for design calculations is 250 kmol/h (10.5 ton/h) of EO fed. Because all EO is consumed stoichiometrically with CO_2, the chemical consumption of CO_2 is also 250 kmol/h (11 ton/h), but the CO_2 feed is approximately 1% greater than 250 kmol/h due to the purge effects in the two recycle loops of Figure 1c. The DMC plant is conceived as an "opportunistic" small project that must be situated "next door" to a big and durable producer of low-cost CO_2, like a typical large coal-Rankine power plant with post-combustion capture by aqueous ethanolamines. Pressure at the top of the CO_2 stripper column in the capture plant is normally below 2 bar. In other words, it is conceivable that such plants export CO_2 as a low pressure gas across short distances. Therefore, the CO_2 stream is assumed available at battery limits of the DMC plant as a low pressure gas at 5 bar and 35 °C. EO is pumped directly to Reaction 1 as a liquid from a storage sphere with saturated liquid EO at 3 bar at ambient temperature. The chemical sequestration of CO_2 (CSC) is equal to 250 kmol/h minus all equivalent CO_2 released in purges, heat, and power consumptions. A negative CSC implies that the process generates (equivalent) CO_2 emissions greater than the CO_2 chemical consumption.

Chemical Reaction Section. As shown in Figure 1c and d, there is a two-phase high-pressure plug-flow reactor (PFR) for Reaction 1 and a liquid-phase low-pressure PFR for Reaction 2. Reaction 1 produces EC from EO and CO_2 at 39.5 bar and 100 °C.[5,8] Thus, a compression section with two stages (Figure 1d) is necessary to feed CO_2 from battery limits at 5 bar to the conditions of Reaction 1. There is an intercooler after stage 1 of compression, but the effluent from stage 2 is not cooled due to the high temperature needed in Reaction 1. The simulation flowsheet for the reaction section of IR in Figure 1d is shown in Figure S1 of the Supporting Information. Approximately 25% excess supercritical CO_2 is employed to guarantee 100% EO conversion with 100% selectivity. The excess of CO_2 is recovered between Reaction 1 and Reaction 2 by a phase separator and recycled back to Reaction 1. Despite its industrial utilization since the 1950s and its previous investigation by several authors,[5,8] there is no rate formula in the literature for Reaction 1 probably because it is a fast and typically irreversible chemical reaction that even does not have side competing reactions.[8] Because a rate formula must be defined for reactor analysis within ASPEN−HYSYS, it is herein adopted that Reaction 1 has a forward rate of second order, which is fast enough to guarantee complete conversion of EO with CO_2 in excess. The kinetic constant for the rate of Reaction 1 was chosen 30 times greater than the corresponding kinetic constant in the forward rate of Reaction 2 (eqs 3 and 4). Thus, the rate of Reaction 1 is expressed as shown in eqs 1 and 2:

$$r_{EO} = k_0 C_{EO} C_{CO_2} \quad (1)$$

dx.doi.org/10.1021/sc400279n | ACS Sustainable Chem. Eng. 2014, 2, 62−69

$$k_0 = 39.7\exp\left(\frac{-13060}{RT}\right) \quad (2)$$

where r_{EO} represents the reaction rate of EO (mol/L min); C_{EO} and C_{CO_2} are concentrations of EO and CO_2 (mol/L), respectively. The activation energy in eq 2 is given in J/mol.

Reaction 2 converts EC with excess MeOH to DMC and EG in equimolar ratios at 1 bar and 40 °C in liquid phase. The unconverted MeOH and EC are recovered in the separation section, but only MeOH is recycled to Reaction 2 (Figure 1c). Rate formulas[1] for Reaction 2 are given by eqs 3 and 4:

$$r_{EC} = k_{+1}C_{EC}C_{MeOH} - k_{-1}\frac{C_{EG}C_{DMC}}{C_{MeOH}} \quad (3)$$

$$k_{+1} = 1.32466\exp\left(\frac{-13060}{RT}\right),\ k_{-1} = 15022\exp\left(\frac{-28600}{RT}\right) \quad (4)$$

where r_{EC} represents the net reaction rate of EC (mol/L min); C_{EC}, C_{MeOH}, C_{EG}, and C_{DMC} are concentrations of EC, MeOH, EG, and DMC (mol/L), respectively. Activation energies are given in J/mol.

The chemical reaction section of IR operates with 100% atom economy and no wastes, that is, side reactions are negligible. This is impressive, but there are some reasons for this. First, in Reaction 1, CO_2 is a very stable and nonreactive molecule. On the other side, EO a very reactive one, which in the absence of other species cannot react or degrade via side reactions. EO also cannot react alone or with itself without promoters because its storage is stable as a liquid in spheres at ambient temperature and 3 bar. EO only reacts alone or with itself in special catalytic cases in a high-temperature gas phase to acetaldehyde or in liquid phase under cationic or anionic catalysis to polyethyleneglycols. Because the conditions of Reaction 1 (liquid phase, 39.5 bar, 100 °C, 25% excess CO2) do not allow any other reactant and are not compatible with isomerization or polimerization scenarios, EO can only proceed to produce EC via a fast reaction with 100% conversion and 100% selectivity. A good deal of the CO_2 excess is recovered and recycled. Second, the subsequent Reaction 2 between EC and MeOH is still slower and also without faster competitors because both species do not react with themselves or degrade in the proposed conditions. Besides, a high excess of MeOH is used (MeOH/EC ≈ 6 mol/mol) simultaneously with low temperature (40 °C) in a large PFR reactor. These conditions imply high selectivity under conversion of 75% per pass without side reactions. The price that has to be paid is a huge separation system that has to break an azeotrope, recover the excess of MeOH, and isolate the products. Unconverted EC is not recycled because it is also a saleable substance, which is easily separated. Thus, it is no wonder that 100% atom economy is possible here. All produced substances—EC, DMC, and EG—are negotiable commodities, and unconverted MeOH is kept in the Reaction 2 loop without losses thanks to the separation section.

Separation Section: Extractive Distillation and Entrainer Selection. It is worth noting that IR presents a separation challenge in the cut of the azeotropic pair DMC−MeOH, which must recover cost effectively all MeOH used in excess in the slow Reaction 2. Extractive distillation (ExD) is the suited separation scheme. The choice of entrainer strongly impacts ExD performance.[2] The entrainer must qualify in three aspects: (i) It must remain in liquid phase (i.e., nonvolatile). (ii) It must change drastically and asymmetrically with liquid-phase activity coefficients of the azeotropic pair. (iii) It must not entail severe HSE issues. Hsu et al.[4] recommend three species as entrainer for this ExD: aniline, phenol, and EG. From the process and HSE points of view, EG is a more attractive option because it is less hazardous and already exists in the effluent from Reaction 2. In a similar work, Matsuda[9] recommends MIBK as a better entrainer than 2-ethoxyethanol. Following these authors, the present study compares the performances of MIBK and EG as entrainers for the ExD of the azeotropic pair DMC−MeOH. This defines two IR process alternatives: IR−MIBK (MIBK as entrainer) and IR−EG (EG as entrainer).

Thermodynamic Properties and Vapor−Liquid Equilibrium (VLE) Calculations. Thermodynamic modeling is decisive in the design of separation systems like ExD trains. Design of Reaction 1 also depends on such models for high-pressure VLE and density calculations, which influence reaction kinetics via liquid-phase concentrations of species. The literature presents calibrated VLE models for some binary systems of interest in the IR context.[4,9,10] Such models normally couple a solution theory (ST) for the liquid phase (e.g., UNIQUAC or Wilson) with an equation of state (EOS) for the vapor phase (e.g., Redlich−Kwong (RK) or Peng−Robinson (PR)). Calibration is critical for ST via the adjustment of its binary interaction parameters (BIPs) with VLE data. On the other hand, BIPs of EOS have much less importance and can be used as zero, especially if the EOS is applied only on the vapor phase as is the case here. In all low pressure sections of IR−MIBK and IR−EG, the BIPs of PR−EOS and RK−EOS are irrelevant and were set to zero. Only in Reaction 1 of both IR−MIBK and IR−EG do the EOS BIPs have some limited importance, but they were also set to zero because the EOS is applied on the vapor phase, while the reaction occurs in the liquid, which is modeled by a calibrated ST. Because the choice of entrainer for ExD directly affects the thermodynamic modeling, two pairs of ST−EOS were adopted here as shown in Table 1, namely, (i) UNIQUAC−RK for all systems without MIBK, i.e., with MeOH−DMC−EC−EG−EO−CO_2, and (ii) Wilson−PR for systems with MIBK−MeOH−DMC only because reliable UNIQUAC BIPs were not found for this trio. Thus, the reaction section and the entire separation section of IR−EG employ UNIQUAC−RK.[4,10] This is also the case for the reaction section and *ordinary* distillations of IR−MIBK, whereas the ExD train of IR−MIBK employs Wilson−PR.[9] The assignment of different thermodynamic models to different sections of ASPEN−HYSYS flowsheets is not problematic and is a common tactical resource. Figure 2 depicts binary TXY−VLE data[4,9,10] at 1 atm for systems MeOH−DMC, MeOH−EC, and DMC−EC, which are plotted against TXY−VLE predictions by UNIQUAC−RK and Wilson−PR with BIPs from Table 1. It is clear that MeOH−DMC has a minimum boiling point azeotrope between 80% and 85% mol MeOH, which is correctly recognized by both UNIQUAC−RK and Wilson−PR. In general, VLE predictions adhere reasonably to data in all cases. UNIQUAC−RK was used in Figure 2a (MeOH−DMC), b (DMC−EC), and c (MeOH−EC), whereas Wilson−PR was used in Figure 2d (MeOH−DMC), e (DMC−EC), and f (MeOH−EC).

Table 1. VLE Models and BIPs for IR−MIBK[9] and IR−EG[4,10]

Reaction section and ordinary distillations of IR−MIBK. Reaction section and all distillations of IR−EG UNIQUAC BIPs for liquid phase [vapor via RK−EOS].

	i = DMC	i = MeOH	i = MeOH	i = CO_2	i = DMC
	j = EC	j = EC	j = EG	j = MeOH	j = MeOH
a_{ij}	2.5273	−0.54094	−32.587	131.7089	636.888
a_{ji}	−6.7598	15.892	2.2712	502.1199	36.688

Extractive distillation train of IR−MIBK. Wilson BIPs for liquid phase [vapor via PR-EOS].

	i = MeOH	i = MeOH	i = DMC
	j = DMC	j = MIBK	j = MIBK
a_{ij}	749.69	818.74	130.45
a_{ji}	288.89	54.36	126.80

The efficacy of entrainers MIBK and EG in terms of breakage of the azeotrope MeOH−DMC in the respective ExD columns of IR−MIBK and IR−EG can be appreciated in Figure 3a. Figure 3a depicts profiles of relative volatility MeOH/DMC versus tray number (tray 0 is the top condenser; entrainer is fed on tray 1) in the ExD columns of IR−MIBK and IR−EG, respectively, with entrainers MIBK and EG. Both entrainers shift the relative volatility of MeOH/DMC to values above 1, but the superiority of EG is significant, giving a shorter column with 35 theoretical stages, while ExD with MIBK needs 50 theoretical stages for the same recoveries of MeOH and DMC.

dx.doi.org/10.1021/sc400279n | ACS Sustainable Chem. Eng. 2014, 2, 62−69

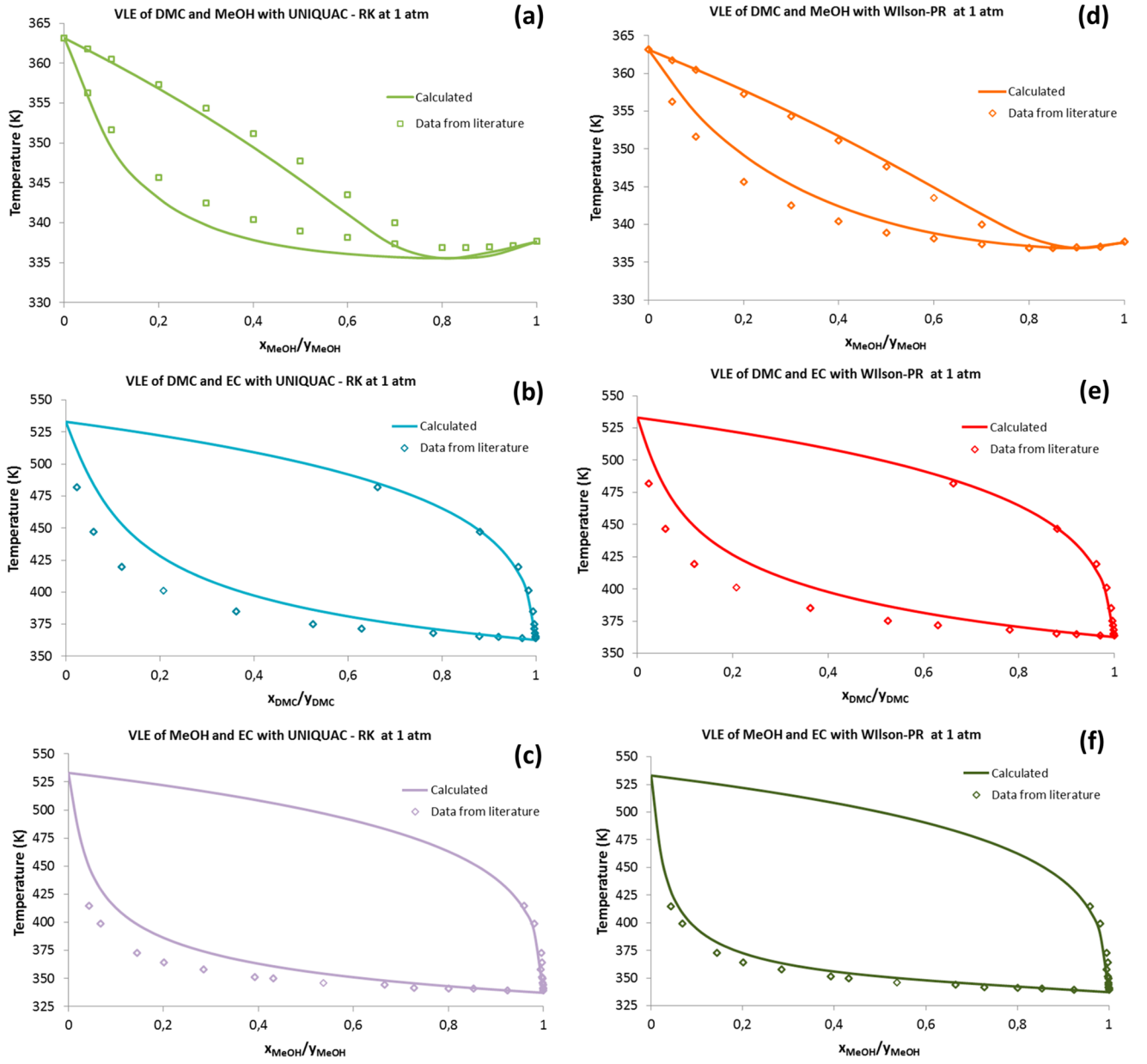

Figure 2. Binary TXY–VLE data at 1 atm versus TXY–VLE predictions with BIPs from Table 1: (a) MeOH–DMC vs UNIQUAC-RK, (b) DMC–EC vs UNIQUAC–RK, (c) MeOH–EC vs UNIQUAC–RK, (d) MeOH–DMC vs Wilson–PR, (e) DMC–EC vs Wilson–PR, and (f) MeOH–EC vs Wilson–PR.

Design of Reaction Sections of IR–MIBK and IR–EG. Both reaction sections have the same design and were calculated with the same VLE model UNIQUAC–RK (Table 1). Figure 1d and Figure S1 of the Supporting Information presents the simulation flowsheet for this common section. It comprehends a CO_2 compression train with two serial compressors, a PFR for Reaction 1 (PFR-100), and a second PFR for Reaction 2 (PFR-101). Fang et al.[1] present equilibrium conversions of EC in Reaction 2 at different conditions of [MeOH]/[EC] mol ratio, reaction temperature, and catalyst concentration. Sensitivity analyses in Figure 3b and c were performed via process simulations to find out the most suitable reactant ratio [MeOH]/[EC] and temperature for Reaction 2. In Figure 3b, the sensitivity analysis recommends a [MeOH]/[EC] ratio of approximately 6, as it combines satisfactorily high EC conversion with not extremely high recycle flow rate of MeOH. Conversely, in Figure 3c, increasing temperature reduces the equilibrium yield of DMC, as expected in exothermic reactions.[1] Thus, in order to avoid unnecessary slowing of kinetics, the temperature of Reaction 2 was chosen at 40 °C as stated previously. Just after Reaction 1, there is a phase separator where excess CO_2 is recovered as the top product and recycled back to Reaction 1,whereas all EC is recovered in the bottom due to its low solubility in supercritical CO_2.[5] Hence, EC is easily separated from the supercritical phase without unnecessary depressurization of CO_2. The EC effluent of Reaction 1 (with some dissolved CO_2) is expanded to 1 bar before entering Reaction 2, which operates at 40 °C and 1 bar. The liquid effluent from Reaction 2 containing MeOH, DMC, EG, and unconverted EC goes to the separation section. The conversions of Reactions 1 and 2 are approximately 100% and 75%, respectively. The PFR designs of Reactions 1 and 2 are shown in Table S1 of the Supporting Information.

Design of Separation Sections of IR–MIBK and IR–EG. The separation sections of IR–MIBK and IR–-EG are similar in terms of operation. The only difference corresponds to the ExD entrainers. IR–MIBK uses MIBK, whereas IR–EG uses EG, with the respective VLE models segregated according to Table 1. Figures S2 and S3 of the Supporting Information depict the respective simulation flowsheets for

dx.doi.org/10.1021/sc400279n | ACS Sustainable Chem. Eng. 2014, 2, 62–69

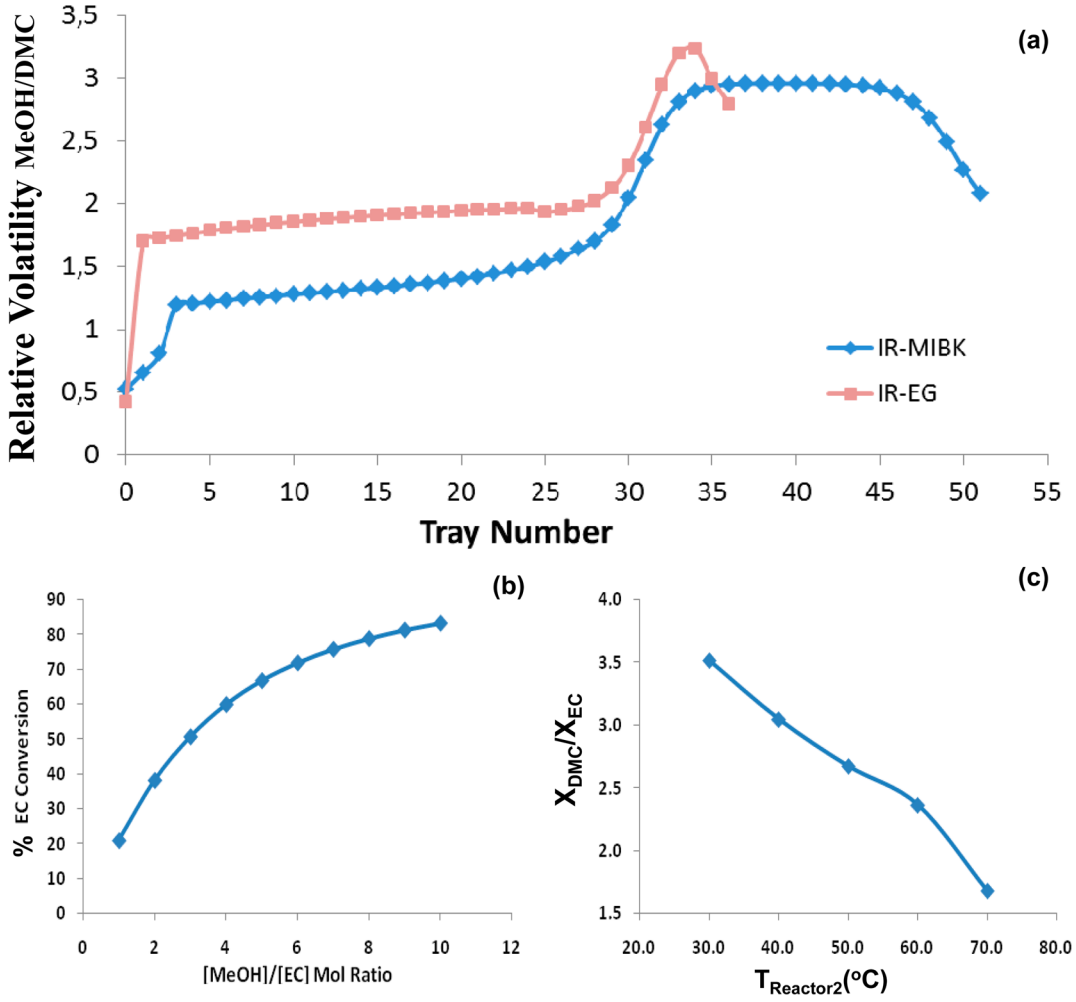

Figure 3. (a) Relative volatility MeOH/DMC profiles in ExD columns of IR−MIBK and IR−EG, respectively, with entrainers MIBK and EG. (b) Influence of [MeOH]/[EC] mol ratio on %EC conversion in Reaction 2 at 40 °C and 1 bar. (c) Influence of temperature on DMC/EC mol ratio in Reaction 2 at 1 bar and [MeOH]/[EC] = 6.

the separation sections of IR−MIBK and IR−-EG. The main design and operational parameters (column pressure, reflux ratios, reboiler duties, recoveries, theoretical stages, etc.) of the separation sections of IR−MIBK and IR−EG are condensed in Table S2 of the Supporting Information. Subatmospheric distillation was selected in some columns to avoid thermal decomposition thresholds of EG (166 °C).

Only the separation section of IR−MIBK is described here with some detail because IR−EG works similarly as shown in Figures S2 and S3 of the Supporting Information. The mechanism used by both ExD columns of IR−MIBK and IR−EG to change the unitary azeotropic relative volatility MeOH/DMC is evidenced in Figure 3a, which shows successful extractive profiles of relative volatility MeOH/DMC with entrainers MIBK and EG separately. IR−MIBK comprehends two ordinary distillation columns and two columns in the upper ExD train with entrainer MIBK. Subatmospheric ordinary column T-100 receives the effluent from Reaction 2 and cuts it between DMC and EG, producing a top distillate with all MeOH and DMC and a bottom with all EG and EC. The top distillate of T-100 is sent as a vapor to the middle of ExD column T-101, which is also fed with recycled liquid MIBK at tray 1. MeOH is distillated (carrying some DMC) as the top product and returned to Reaction 2. Feeding T-101 with vapor distillate from T-100 reduces the reboiler duty of T-101, improving the economics of the ExD train. The bottom product of ExD T-101 is sent to column T-103, which produces 99.5 wt % DMC as the top distillate and regenerated MIBK as the bottom product to be recycled to tray 1 of ExD T-101. The bottom product of T-100 is sent to the subatmospheric column T-102, where EG is recovered as the top distillate, and EC is the bottom product, both at temperatures below the respective thermal decomposition thresholds.

RESULTS AND DISCUSSION

Energy Consumption and Environmental Impact Analysis. The environmental performance analysis of alternatives IR−MIBK and IR−EG involves the assessment of efficiency of energy usage (in terms of power and heat consumption) and environmental impact assessment. As shown in Figure 4a and b, the heat consumption of distillations reach approximately 57 and 53 MW (7% less for the later), while the power consumption of compressors and pumps reach approximately 619 and 641 kW, respectively, for IR−MIBK and IR−EG. Table S2of theSupporting Information shows that almost two-thirds of the heat consumption of both IR−MIBK and IR−EG are associated with the ExD trains for separation of the azeotropic pair DMC−MeOH.

Heat integration of columns (HIC) in both separation trains is not a standard option and is not always feasible. HIC always aggregates more CAPEX in equipment and control systems and several start-up and controllability issues. Besides, in the present case, temperature distributions is similar in all columns, and some of them do not allow higher operating pressures (e.g., EG columns). Columns have similar temperature profiles due to

dx.doi.org/10.1021/sc400279n | ACS Sustainable Chem. Eng. 2014, 2, 62−69

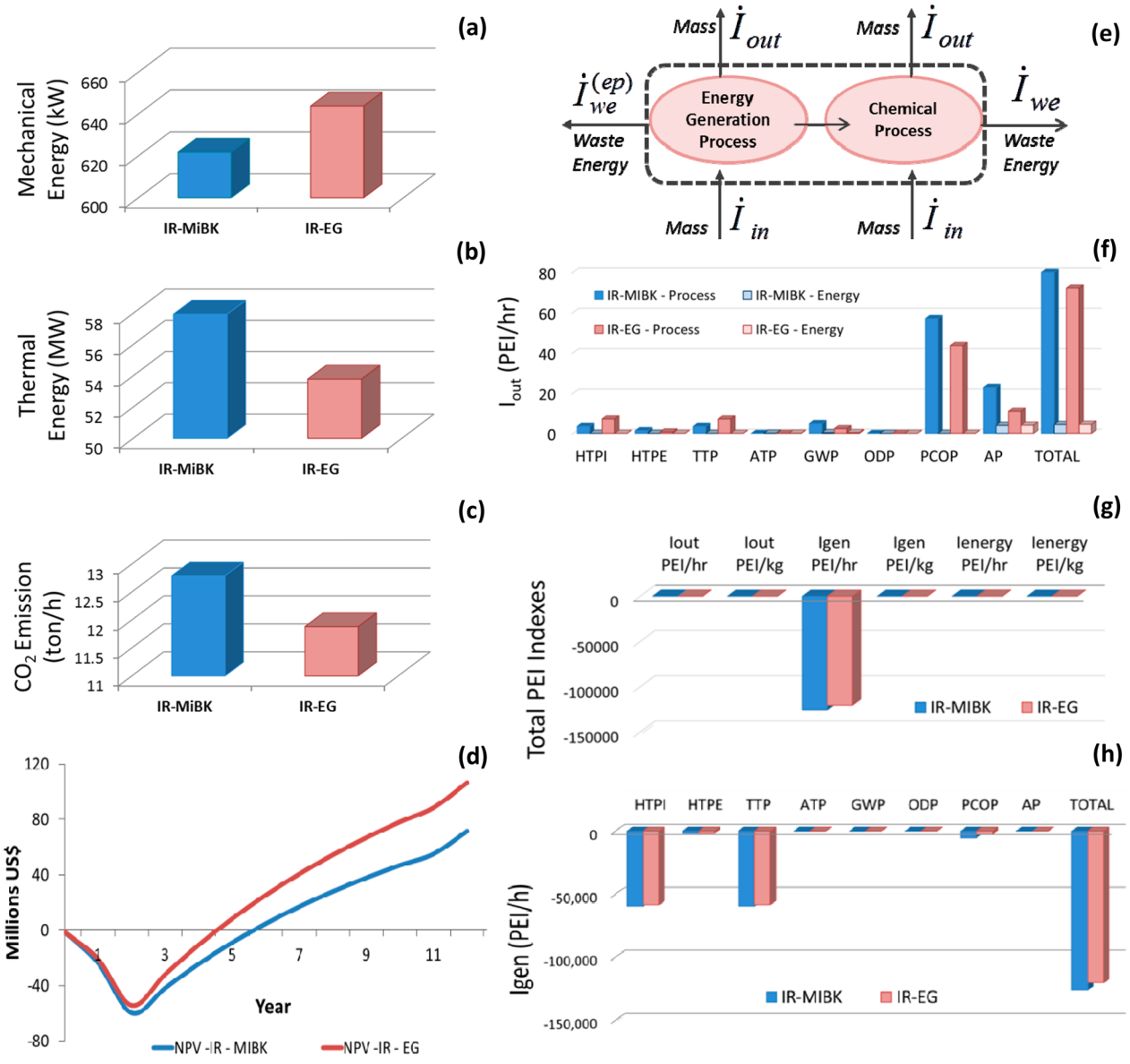

Figure 4. IR–MIBK versus IR–EG: (a) power consumption (kW), (b) heat consumption (MW), (c) CO_2 emissions (ton/h), (d) NPV vs year (10^6 US$), (e) overall mass and PEI balances for chemical and energy generation processes, (f) $\dot{I}_{out}$ total output rate of PEI, (g) total PEI indexes, and (h) $\dot{I}_{gen}$ rate of creation (or consumption if negative) of PEI.

subatmospheric operation of EG columns, which imposes top or bottom temperatures near the thermal threshold of EG (165 °C). IR columns also have very different internal vapor flow rates (Table S2, Support Information). The ExD columns have much higher vapor flow than other columns. This is another obstacle to heat integration between them. The only feasible HIC involves replacing the single ExD column with a bipartite (tripartite) configuration where two (three) smaller ExDs are coupled at different pressures with a common condenser–reboiler between them. In this case, HIC is possible for IR–MIBK only (this is unfeasible for IR–EG due to EG decomposition issues) reducing ExD heat duty in 50% (66.7%). In the present case, the only aspect of HIC that was observed was to send the top product of column T-100 as a vapor to ExD T-101, but this also has implications in column pressures. Both ExD trains also allocate the biggest columns (both in terms of height and diameter) in the respective separation sections. This is a portrait of the energy burden imposed to circumvent the azeotropic obstacle in order to attain MeOH–DMC specifications. In summary, HIC is not a straightforward matter and is beyond the present scope, but it is an interesting resource that opens great opportunities for reducing OPEX and CO_2 emissions. The implications of HIC in DMC production from CO_2 will be the object of future work.

A comparative analysis of Figure 4a and b reveals that IR–MIBK is less energy efficient than IR–EG. Consequently, this is inversely posed in terms of CO_2 emissions of both processes. The conversion of heat and power consumptions of IR–MIBK and IR–EG in equivalent GHG emissions is accomplished with Table S3 of the Supporting Information from CEQR–NYC.[11] With this table and Figure 4a and b, one obtains equivalent CO_2 emissions of IR–MIBK and IR–EG in Figure 4c as approximately 12.6 ton/h and 11.7 ton/h, respectively, both greater than the chemical consumption of CO_2 of 11 ton/h.

dx.doi.org/10.1021/sc400279n | ACS Sustainable Chem. Eng. 2014, 2, 62–69

In fact, processes IR−MIBK and IR−EG are not truly equivalent in terms of production of DMC. Despite the fact that IR−MIBK and IR−EG share the same reactor designs in Reactions 1 and 2 (Table S1,Supporting Information) and the same consumptions of EO and CO_2 (Table 2), the differences

Table 2. Economical and Environmental Performances of DMC Production

performance Index	IR−MIBK	IR−EG
DMC production (kton/year)	134.4	130.6
EC production (kton/year)	52.2	58.7
EG production (kton/year)	92.7	94.1
EO consumption (kton/year)	91.7	91.7
CO_2 consumption (kton/year)	92.7	92.7
MeOH consumption (kton/year)	95.2	93.3
CO_2 equiv. emissions (kton/year)	106.2	98.6
CSC[a] (kton/year)	−15.9	−8.1
CO_2 emission reduction (%)	85%	92%
NPV (10^6 US$)	71.5	106.5
PBP (years)	5.5	4.5

[a]CSC = chemical sequestration of CO_2 = CO_2 consumed [reaction] − CO_2 emitted [heat, power. and purges].

in the separation trains vis à vis MeOH recycles allowed IR−MIBK to operate Reaction 2 with a slightly higher MeOH/EC ratio. This gives a higher DMC production of 134.4 kton/year, while the corresponding production of IR−EG is 2.8% less or 130.6 kton/year. For the same reason, MeOH consumptions and EC exportations are different for IR−MIBK and IR−EG. As shown in Table 2, the later consumes 93.3 kton/year of MeOH and produces 58.7 kton/year of EC, while IR−MIBK consumes 95.2 kton/year of MeOH and produces 52.2 kton/year of EC.

The chemical sequestration of CO_2 (CSC) is given by the reactive consumption of CO_2 (11ton/h) minus all equivalent releases of CO_2 in purges, heat, and power. Table 2 and Figure 4c show that CSC is negative for IR−MIBK and IR−EG, reaching −15.9 and −8.1 kton/year, respectively. In other words, CO_2 emissions overcome the chemical conversion of CO_2 in both cases. The energetic burden to separate DMC−MeOH is a major underlying reason for this negative CSC in IR−MIBK and IR−EG. As consolation, Table 2 shows that there are abatements of emitted CO_2 of 85% and 92% in IR−MIBK and IR−EG, respectively, thanks to its chemical conversion to DMC and EC.

The environmental impact assessment of IR−MIBK and IR−EG can be addressed via the life cycle analysis, exergy analysis, and waste reduction (WAR) algorithm.[12] The last method is based on potential environmental impact (PEI) balances via mass/energy streams entering/leaving the chemical process and its energy generation process (Figure 4e). The rates of PEI associated with waste energy lost by the chemical and energy generation processes are small compared to the total input/output rates of PEI and are neglected.[12] Steady-state PEI conservation is written in eq 5[12]

$$\dot{I}_{outf} = \dot{I}_{in} + \dot{I}_{gen} \tag{5}$$

where $\dot{I}_{in}$ and $\dot{I}_{out}$ are the total input and output rates of PEI, respectively, for the chemical process as well for the energy generating process or for both taken together, and $\dot{I}_{gen}$ is the rate at which PEI is created/destroyed by chemical reactions. It is worth noting that a PEI consuming process has negative $\dot{I}_{gen}$, therefore contributing to removal of hazardous substances from the environment. The rates of input and output of PEI are calculated according to eqs 6 and 7

$$\dot{I}_{in} = \sum_i \alpha_i \dot{I}_{i,in} = \sum_i \alpha_i \sum_j \dot{M}_{j,in} \sum_k x_{kj} \psi_{ki}^S \tag{6}$$

$$\dot{I}_{out} = \sum_i \alpha_i \dot{I}_{i,out} = \sum_i \alpha_i \sum_j \dot{M}_{j,out} \sum_k x_{kj} \psi_{ki}^s \tag{7}$$

where α_i is the weighting factor of PEI category i, $\dot{M}_{j,in}$ ($\dot{M}_{j,out}$) is the mass flow rate of j^{th} input (output) stream; $x_{k,j}$ is the mass fraction of component k in j^{th} input (output) stream, and ψ_{ki}^s is the specific PEI of category i related to species k. WAR considers eight PEI categories: human toxicity potential by ingestion (HTPI), human toxicity potential by exposure (HTPE), terrestrial toxicity potential (TTP), aquatic toxicity potential (ATP), global warming potential (GWP), ozone depletion potential (ODP), photochemical oxidation—or smog formation—potential (PCOP), and acidification—or acid rain—potential (AP).[12] Figure 4f, g, and h display WAR results for IR−MIBK and IR−EG, with uniform weighting (α_i = 1, $\forall i$) and considering the energy generating process. Figure 4f shows the PEI output index $\dot{I}_{out}$ for all categories. GWP, PCOP, and AP have the most relevant contribution to the total output PEI, with IR−MIBK displaying a slightly worse PEI performance compared to IR−EG, albeit the best HTPI and TTP results belong to IR-MIBK. IR−MIBK has also higher GWP than IR−EG, confirming results of CO_2 emissions from energy requirements in Figure 4a, b, and c. Figure 4g presents total PEI indexes with similar (almost zero) results for both IR−MIBK and IR−EG (label "energy" refers to energy generating process), which were eclipsed by strongly negative $\dot{I}_{gen}$ for both processes but slightly more negative for IR−MIBK. Both $\dot{I}_{gen}$ are highly negative because IR−MIBK and IR−EG are great "devourers" of PEI because both are fed with hazardous EO and MeOH (with very high specific scores in PEI categories HTPE, TTP, and PCOP, in the WAR database), returning less HSE problematic DMC, EC, and EG. The reason why $\dot{I}_{gen}$ is slightly more negative for IR−MIBK is shown in Table 2. IR−MIBK is more effective as a replacer of dangerous MeOH by less hazardous DMC (albeit at expense of a 7% higher consumption of heat). In Figure 4h, the PEI creation rate $\dot{I}_{gen}$ is detailed for all categories. With the exception of some indexes slightly positive or negative (e.g., AP, etc.), the creation rates of HTPI, TTP, and PCOP are strongly negative due to high consumptions of EO and MeOH. In general, IR−MIBK and IR−EG present similar results in Figure 4h, mainly because they operate the same chemical reactions with similar conversions and recycle loops.

Economic Analysis. Analyses of IR−MIBK and IR−EG follow Turton et al.[13] to estimate capital (CAPEX) and operation expenditures (OPEX) with data imported from process simulations and designs generated by ASPEN−HYSYS.[14] To compare process alternatives, the respective net present value (NPV) and payback period (PBP) are determined with CAPEX, OPEX, and revenues.[13] In order to assess NPV−PBP, the following parameters were chosen: (i) working capital, 5% of CAPEX; (ii) operating charge, 15% of labor cost; (iii) plant overhead, 25% of labor and maintenance costs; (iv) rate of return, 8% per year; (v) tax rate, 40% per year; (vi) salvage value, 20% of CAPEX; (vii) depreciation method, straight line; (viii) project capital, raw material, product, and utility escalations set at 3.5% per year; (ix) prices

of EO, MeOH, DMC, EG, EC, MIBK, and low pressure CO_2 (ICIS pricing) are 1740, 670, 950, 1600, 1700, 2210, and 3 US $/ton, respectively; and (x) utility costs as in Table S4 of the Supporting Information). NPV profiles for IR−MIBK and IR−EG are depicted in Figure 4d, showing that IR−MIBK and IR−EG have PBPs of 5.5 and 4.5 years, respectively. Table 2 shows the NPVs at the 12th year of project life as US$ 71.5×10^6 and US$ 106.5×10^6 for IR−MIBK and IR−EG, respectively. Table 2 summarizes NPV−PBP results and productions/consumptions of DMC, EG, EC, EO, MeOH, CO_2, and CSC. The CO_2 abatement indexes, PEI (GWP, PCOP, AP, and total) output indexes, Figure 4a, b, c, and NPV−PBP imply that IR−EG is the best alternative. It is more profitable and more sustainable (inferior GHG releases, inferior PEI output indexes, inferior consumption of energy, and higher CSC). Moreover, IR−EG is less HSE problematic because EG is less hazardous than MIBK.

Final Remarks. Production of DMC via an indirect route (IR) was evaluated aiming to assess energy efficiency, CO_2 emissions, potential environmental impact (PEI), and profitability. Two processing alternatives, IR−MIBK and IR−EG, using, respectively, MIBK and EG as entrainers in the extractive distillation (ExD) for the azeotropic pair DMC−MeOH were assessed according to the metrics above. On the basis of simulation and design results, both IR−MIBK and IR−EG have high OPEX due to heat consumption, and two-thirds of it is associated with the energy sink to separate DMC−MeOH via ExD. IR−MIBK and IR−EG are similar processes with similar PEI indexes, GWP, PCOP, and AP, with a perceptible advantage in favor of IR−EG. The differences between IR−MIBK and IR−EG are more visible in terms of energy consumption, CSC, and profitability. Both are profitable (based on chosen market prices) with payback periods of 5.5 and 4.5 years but gave negative indexes of chemical sequestration of CO_2 (CSC). That is, in both alternatives, the chemical consumption of CO_2 for DMC production was overcome by CO_2 emissions, mainly from the separation system. Amid this desolating scenario, IR-EG exhibited superior sustainability and economic indexes: lower heat consumption, best PEI indexes, chemical abatement of 92% of the emitted CO_2, and higher NPV. IR-EG is also superior to IR−MIBK in terms of HSE issues.

■ ASSOCIATED CONTENT

Supporting Information

Figure S1: Simulation flowsheet for the reaction section of IR-MIBK and IR-EG (DMC production). Figure S2: Simulation flowsheet for the separation section of IR-MIBK (DMC production). Figure S3: Simulation flowsheet for the separation section of IR-EG (DMC production). Table S1: PFR designs for reaction 1 and reaction 2. Table S2: Design of the separation sections of IR-MIBK and IR-EG (DMC production). Table S3: Equivalence factors; energy production and emitted CO_2.[11] Table S4: Utility Costs for DMC Production. This material is available free of charge via the Internet at http://pubs.acs.org.

■ AUTHOR INFORMATION

Corresponding Author

*Tel.: +55-21-2562-7535. Fax: +55-21-2562-7637. E-mail: jlm@eq.ufrj.br.

Notes

The authors declare no competing financial interest.

■ ACKNOWLEDGMENTS

Authors acknowledge CNPq-Brazil, FAPERJ-Brazil, and CAPES-Brazil Grant 113/2008 for financial support.

■ REFERENCES

(1) Fang, Y. J.; Xiao, W. Experimental and modeling studies on a homogeneous reactive distillation system for dimethyl carbonate synthesis by transesterification. *Sep. Purif. Technol.* **2004**, *34* (1−4), 255−263.

(2) Nisoli, A.; Bouwens, S. M.; Doherty, M. F.; Malone, M. F. Method of Separating Dimethyl Carbonate and Methanol. U.S. Patent 6315868 B1, November 13, 2001.

(3) Cui, H.; Wang, T.; Wang, F.; Gu, C.; Wang, P.; Dai, Y. Kinetic study on the one-pot synthesis of dimethyl carbonate in supercritical CO_2 conditions. *Ind. Eng. Chem. Res.* **2004**, *43* (24), 7732−7739.

(4) Hsu, K.; Hsiao, Y.; Chien, I. Design and control of dimethyl carbonate-methanol separation via extractive distillation in the dimethyl carbonate reactive-distillation process. *Ind. Eng. Chem. Res.* **2010**, *49* (2), 735−749.

(5) Sakakura, T.; Choi, J.; Yasuda, H. Transformation of carbon dioxide. *Chem. Rev.* **2007**, *107*, 2365−2387.

(6) *IPCC Special Report on Carbon Dioxide Capture and Storage*. Metz, B., Davidson, O., Coninck, H., Loos, M., Meyer, L., Eds.; Prepared by Working Group III of the Intergovernmental Panel on Climate Change, 2005. www.ipcc.ch/pdf/special-reports/srccs/srccs_wholereport.pdf

(7) Wang, J.-Q.; Sun, J.; Shi, C. Y.; Cheng, W. G.; Zhanga, X. P.; Zhang, S. J. Synthesis of dimethyl carbonate from CO_2 and ethylene oxide catalyzed by K_2CO_3-based binary salts in the presence of H_2O. *Green Chem.* **2011**, *13*, 3213−3217.

(8) Peppel, W. J. Preparation and properties of the alkylene carbonates. *Ind. Eng. Chem.* **1958**, *50* (5), 767−770.

(9) Matsuda, H.; Takahara, H.; Fujino, S.; Constantinescu, D.; Kurihara, K.; Tochigi, K.; Ochi, K.; Gmehling, J. Selection of entrainers for the separation of the binary azeotropic system methanol + dimethyl carbonate by extractive distillation. *Fluid Phase Equilib.* **2011**, *310* (1−2), 166−181.

(10) Camy, S.; Condoret, J. S. Dynamic modeling of a fractionation process for a liquid mixture using supercritical carbon dioxide. *Chem. Eng. Process.* **2003**, *40* (6), 499−509.

(11) City Environmental Quality Review (CEQR) Technical Manual. New York City Mayor's Office of Environmental Coordination, 2012. http://www.nyc.gov/html/oec/downloads/pdf/2012_ceqr_tm.

(12) Cabezas, H.; Bare, J. C.; Mallick, S. K. Pollution prevention with chemical process simulators: The generalized waste reduction (WAR) algorithm—Full version. *Comput. Chem. Eng.* **1999**, *23*, 623−634.

(13) Turton, R.; Bailie, R. C.; Whiting, W. B.; Shaeiwitz, J. A. *Analysis, Synthesis, and Design of Chemical Processes*, 3rd ed.; Prentice Hall: Upper Saddle River, NJ, 2009.

(14) *HYSYS® 2004.2, User Guide*. Aspen Technology, Inc.: Burlington, MA, 2005.